



Contents lists available at ScienceDirect

Science of the Total Environment

journal homepage: www.elsevier.com/locate/scitotenv

Ecological degradation of a fragile semi-arid wetland and the implications in its microbial community: The case study of Las Tablas de Daimiel National Park (Spain)

Esther Santofimia^{a,*}, Elena González-Toril^b, Graciela de Diego^b, Blanca Rincón-Tomás^a, Ángeles Aguilera^{b,1}

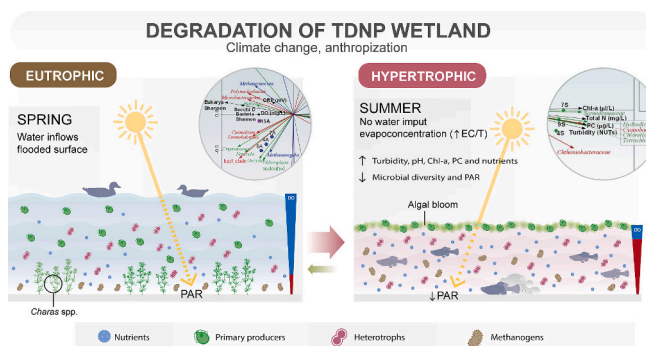
^a Instituto Geológico y Minero de España - Consejo Superior de Investigaciones Científicas (IGME-CSIC), Ríos Rosas, 23, 28003 Madrid, Spain

^b Centro de Astrobiología (CAB), CSIC-INTA, Carretera de Ajalvir km4, 28850 Torrejón de Ardoz, Madrid, Spain

HIGHLIGHTS

- Seasonal changes influence water physico-chemical variations and microbial community
- *Tolypothrix*, unclassified Cyanobacteria and mainly alga *Hydrodictyon* cause the formation of the phytoplankton bloom
- Phytoplankton bloom reduces microbial diversity and changes its composition
- Increase in Chl-a and nutrient values causes hypertrophy, indicating the ecological state sustains a degradation
- Climate change and anthropization is leading to a gradual deterioration of this fragile semi-arid wetland

GRAPHICAL ABSTRACT



ARTICLE INFO

Editor: Fernando Pacheco

Keywords:

Eutrophication
Microbial diversity
Hydromicrobiological approach
Shallow wetland

ABSTRACT

Las Tablas de Daimiel National Park (TDNP, Iberian Peninsula) is a semi-arid wetland of international significance for waterfowl and serves as a migratory route for various bird species. However, TDNP presents strong anthropization and fluctuating water levels, making it a highly fragile ecosystem. Water physico-chemical parameters and microbial diversity of the three domains (Bacteria-Archaea-Eukarya) were analysed in Zone A and Zone B of the wetland (a total of eight stations) during spring and summer, aiming to determine how seasonal changes influence the water quality, trophic status and ultimately, the microbial community composition. Additionally, Photosynthetically Active Radiation (PAR) was used to determine the trophic status instead of transparency using Secchi disk, setting the threshold to 20–40 $\mu\text{mol}/\text{sm}^2$ for benthic vegetation growth. In spring, both zones of the wetland were considered eutrophic, and physico-chemical parameters as well as microbial diversity were similar to other wetlands, with most abundant bacteria affiliated to Actinobacteriota, Cyanobacteria, Bacteroidota, Gammaproteobacteria and Verrucomicrobiota. Methane-related taxa like Methanosarcinales and photosynthetic *Chlorophyta* were respectively the most representative archaeal and eukaryotic groups. In summer, phytoplankton bloom led by an unclassified Cyanobacteria and mainly alga *Hydrodictyon* was

* Corresponding author.

E-mail addresses: e.santofimia@csic.es, e.santofimia@igme.es (E. Santofimia).

¹ These authors contributed equally to this work

<https://doi.org/10.1016/j.scitotenv.2024.171626>

Received 20 November 2023; Received in revised form 7 March 2024; Accepted 8 March 2024

Available online 11 March 2024

0048-9697/© 2024 The Authors. Published by Elsevier B.V. This is an open access article under the CC BY-NC-ND license (<http://creativecommons.org/licenses/by-nc-nd/4.0/>).

observed in Zone A, resulting in an increase of turbidity, pH, phosphorus, nitrogen, chlorophyll-a and phycocyanin indicating the change to hypertrophic state. Microbial community composition was geographical and seasonal shaped within the wetland as response to changes in trophic status. Archaeal diversity decreases and methane-related species increase due to sediment disturbance driven by fish activity, wind, and substantial water depth reduction. Zone B in summer suffers less seasonal changes, maintaining the eutrophic state and still detecting macrophyte growth in some stations.

This study provides a new understanding of the interdomain microbial adaptation following the ecological evolution of the wetland, which is crucial to knowing these systems that are ecological niches with high environmental value.

1. Introduction

Las Tablas de Daimiel National Park (TDNP) is one of the largest semi-arid wetlands in the Mediterranean area as well as a UNESCO Biosphere Reserve since 1980, among several other protection forms (Aguilera et al., 2013). Wetlands are among the ecosystems with the highest biodiversity and biological activity (Dudgeon et al., 2006). These ecosystems are considered to be important carbon sinks and they have a marked influence on climate change (Ward and Tockner, 2001). They also provide a number of local services, including maintaining water quality and supply, regulating atmospheric gases, sustaining unique indigenous biota, and providing cultural, recreational and educational resources, increasing the biodiversity of the whole region (Clarkson et al., 2013; Dise, 2009). However, wetlands are normally worldwide threatened by unsustainable water use, draining of wetlands, discharge of waste or contaminated water, excessive loading of nutrients, and/or pressure due to tourism infrastructure. These situations cause harmful effects like alteration in their hydrogeological characteristics, local extinction of fauna, and destruction of vegetation (van Asselen et al., 2013; Bravo-Martin et al., 2019; Davidson, 2014). To date, about 50 % of the world's original wetland area has been lost, reaching up to >90 % in some European countries (Davidson, 2014).

The TDNP wetland is also grappling with habitat loss, primarily influenced by factors such as global climate change and a strong anthropization. It exhibits pronounced year-on-year fluctuations in its water level, displaying a high degree of water turbidity. Its characteristic benthic vegetation, *Chara* spp., is almost absent, accompanied by an increase in the population of invasive fish species and a significant reduction of Anatidae bird population. These combined changes are leading to a eutrophication of the TDNP (Santofimia et al., 2021).

Eutrophication, a key indicator of aquatic ecosystem degradation, is often assessed through water column parameters (Carlson, 1977; OECD, 1982). This process not only affects water quality but also influences the microbial community in wetlands, with potential consequences for biogeochemical processes (Wang et al., 2022). Characterized by increased nutrients (nitrogen and phosphorus), eutrophication can lead to cyanobacteria proliferation and algal blooms, altering the biogeochemical cycling within the wetland (Li et al., 2020a, 2020b; Sánchez-Carrillo et al., 2014). Furthermore, altered nutrient levels and environmental conditions may foster the rise of specific functional microorganisms involved in both the occurrence and degradation of algal blooms, thereby influencing the distribution of microbial communities (Xie et al., 2020). Hence, the microbial response could be used as an evaluation index for eutrophication (Wang et al., 2022).

Recent studies reveal that the response of microbial communities to environmental changes occurs in a spatially and temporally dynamic manner. However, the majority of these works only present the microbial diversity of one or two domains, lacking a comprehensive and accurate representation of the entire microbial community (Chao et al., 2021; Wang et al., 2022). The present study focuses on a fragile semiarid wetland in the Mediterranean region, investigating how alterations in abiotic/biotic water parameters drive changes in trophic state and subsequently impact the distribution, abundance and composition of microbiological communities of the three domains (Bacteria-Archaea-

Eukarya) within the ecosystem. Thus, our research provides a novel comprehension of interdomain microbial adaptation in response to the ecological evolution of wetlands, offering critical insights into these ecosystems as ecological niches of significant environmental importance.

2. Materials and methods

2.1. Site description

TDNP is located in central Spain (Fig. 1). The wetland is found at the confluence of two rivers, the Guadiana and the Cigüela, in a wide floodplain that constitutes the natural discharge area of the 15,000 km² West La Mancha aquifer, an aquatic ecosystem that serves as an outstanding reservoir for flora and fauna (Moreno and Jiménez, 2013). The brackish water from the Cigüela tributary converges with freshwater from the Guadiana River, and the West La Mancha aquifer discharges.

Due to the scarcity of water in TDNP several initiatives took place to modify the wetland, including the construction of two dams to retain water and maintain a larger extension of flooded surface. One was placed in the final stretch of the fluvial wetland (Puente Navarro dam) and another in the intermediate stretch of the Park (Fig. 1). Our study area is divided in two zones by the Morenillo dam: (1) Zone A, in the upper part of the dam, and (2) Zone B, in the downer part of the dam. Additionally, Zone B is also limited by the Puente Navarro dam in its downstream area (Fig. 1). Representative element photographs of the TDNP wetland are shown in Fig. 2.

2.2. In situ measurements and physico-chemical sampling collection

In 2018, different sampling sites within the wetland were selected for in situ physico-chemical measurements and water sampling during spring in April (1A, 2A, 4A, 7A, 9A, 11A, 12A, 15A, 17A), when the wetland presented >80 % of flooded surface (1020 ha); and during summer, in September (1S, 4S, 7S, 9S, 12S, 13S, 15S, 17S), with a 50 % of flooded surface (575 ha) and a strong reduction of water depth in Zone A. Additionally in April, samples were also taken at the two surface-water inflows of the TDNP, the Cigüela River (E1) and the Guadiana River (E2, G3 and G6) (Fig. 1).

Geographic locations (in UTM coordinates) were obtained using a Garmin GPS model 76S running in differential mode. Depth measurements and vertical profiles of pH, redox potential (ORP), temperature (T), dissolved oxygen (DO), electric conductivity (EC), turbidity, chlorophyll-a (Chl-a), and phycocyanin (PC) were performed by using EXO2 Water Quality Probe (Ysi, USA), and Photosynthetically Active Radiation (PAR) with a Hydrolab DS5 probe (Hach, USA). Transparency measurements were carried out by using a 20-cm diameter Secchi disk (SD). Nutrient concentrations (total N and total P) were measured with a HACH DR2800 spectrophotometer (Iowa, USA) using specific analytical cuvettes (methods LCK 138 for total N and LCK 349 for total P) at the National Park research facilities. Furthermore, two water samples were obtained at each sampling site with a Kemmerer stainless steel bottle of 1.2 L. All samples were filtered in situ with 0.45- μ m-membrane filters

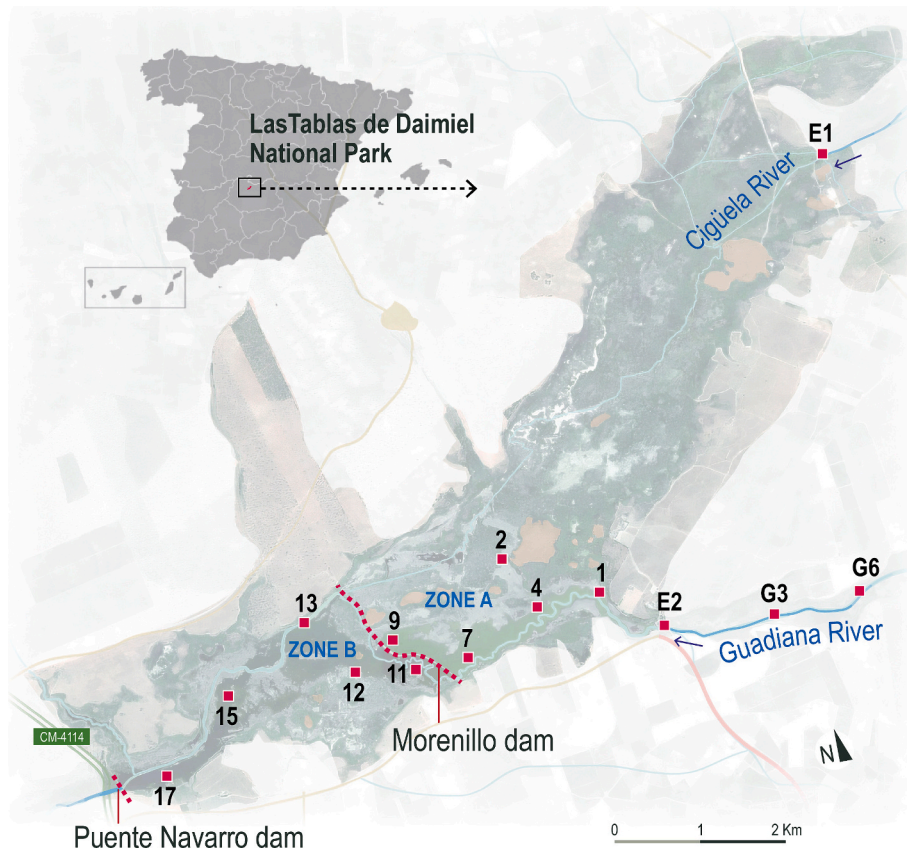


Fig. 1. Las Tablas de Daimiel National Park (TDNP) map, including the location of sampling sites.

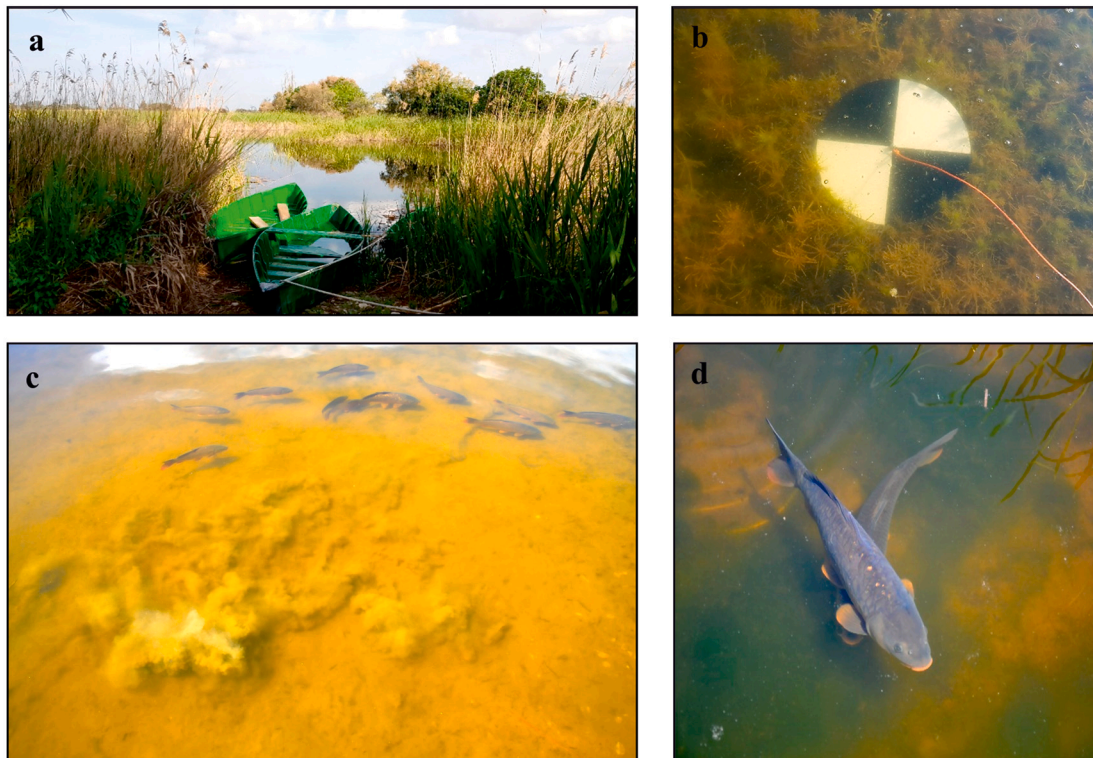


Fig. 2. Representative photographs of TDNP. a View of the wetland. b Development of characteristic benthic vegetation (*Chara* spp.) in Zone B and Secchi disk. c Benthic fish populations stirring up the sediment.. d. Specimen of exotic fish dominating the wetland (*Cyprinus carpio*).

from Millipore (HAWP04700 Merck-Millipore), stored in 125-mL polyethylene bottles, acidified with HNO₃, and stored at 4 °C until further processing.

Total organic carbon (TOC) was determined by means of oxidation by combustion of organic carbon according to method UNE-EN 1484 and detergents via the methyl blue method active substances test (MBAS) and Shimadzu total organic carbon analyzer (TOC-VCPH). Ions such as K⁺, Na⁺, Ca²⁺, and Mg²⁺ were determined by flame atomic emission spectrophotometry (ICP-AES); Cl⁻, SO₄²⁻, NO₃⁻ and NO₂⁻ were determined by ionic chromatography. HCO₃⁻, NH₄⁺, and SiO₂ were determined by continuous flow auto-analyzer absorption spectrophotometry (UV-VIS). Dissolved metals such as Cu, Zn, Se, Cr, Mn, As, Fe, Al, Co, Ba, Ni, U, V, Mo and Sb were analysed through inductively coupled plasma mass spectroscopy (ICP-MS).

2.3. Wetland trophic status classification

Trophic state is an important property of aquatic ecosystems as it reflects the anthropogenic influence on water quality and the ecological functioning of rivers, lakes and wetlands. This study has used the Organization for Economic Cooperation and Development method (OECD, 1982) to classify the wetland according to trophic status in five categories (Table 1Sa). This classification uses chlorophyll-a (Chl-a), total phosphorus (TP) and transparency (measured using SD) as water quality parameters.

2.4. Microbiological sample collection, DNA extraction, amplification and sequencing

For biodiversity characterization, three sampling sites were selected in Zone A (4, 7, 9) and two in Zone B (12, 15). They were sampled in April (4A, 7A, 9A, 12A, 15A) and in September (4S, 7S, 9S, 12S, 15S). Besides, in April three additional sampling sites were selected in the Guadiana River (E2A, G3A and G6A) (Fig. 1). One liter of water was filtered in situ with 0.22-µm membrane filters from Millipore (GTTPO2500 Merck-Millipore) and stored at -20 °C until further processing.

DNA extraction and elution was done according to the manufacturer's instructions. At first, filters were cut into small pieces with a sterile scalpel and introduced into a Lysing Matrix Tube from FastDNA™ SPIN Kit for Soil (MP Biomedicals, LLC). To disrupt cells, three 30s pulses of the FastPrep-24™ 5G Instrument (MP Biomedicals, LLC) at speed 4.0 were performed. DNA was quantified using PICOGREEN®.

Extracted DNA was used in a first PCR of 27 cycles with Q5® Hot Start High-Fidelity DNA Polymerase (New England Biolabs) in the presence of 100 nM primers for 16S V3-V4 region amplification, CS1 (5'-ACACTGACGACATGGTTCTACACCTACG GGNGCGWGCA G-3') and CS2 (5'-TACG GTAGCAGAGACTTGGTCTGAC TACHVGGGTATCTA AT CC-3'). Each sample was amplified and, after the first PCR, a second PCR of 14 cycles was performed with Q5® Hot Start High-Fidelity DNA Polymerase (New England Biolabs) in the presence of 400 nM of primers (5'-AATGATACGGCGACACCGAGATCTACACTGACGACATGTTCTACA-3' and 5'-CAAGCAGAAGACGGCATAACGAGAT-[barcode]-TACGG-TAGCAGAGACT TGGTCT-3') of the Access Array Barcode Library for Illumina Sequencers (Fluidigm). These final amplicons were validated and quantified by an Agilent 2100 Bioanalyzer using DNA7500 chips, and an equimolecular pool of these amplicons was purified by agarose gel electrophoresis to eliminate primers/dimers. This purified pool was then titrated by quantitative PCR using the Kapa-SYBR FAST qPCR kit for LightCycler480 and a reference standard for quantification. Finally, the pool of amplicons was denatured prior being seeded on a flowcell at a density of 10 pM, where clusters were formed and sequenced using a MiSeq Reagent Kit v3 in a 2 × 300 pair-end sequencing run on a MiSeq sequencer (Parque Científico de Madrid, Spain).

The MiSeq sequencer is a high-throughput DNA sequencing platform that plays a crucial role in studying microbial ecology since produces

highly accurate sequencing data, essential for reliable analysis of microbial diversity and community structure, offers sufficient read length, allowing to sequence regions of interest in microbial genomes, such as the 16S rRNA gene, for taxonomic identification. Additionally, its robust sequencing chemistry and data quality contribute to the reproducibility of data, which is crucial for drawing meaningful conclusions and making valid comparisons between samples (Bradley et al., 2016; Tas, 2011).

2.5. OTUs detection and classification

For OTU (Operational Taxonomic Unit) detection and classification, sequence processing and analyses were carried out using Mothur v.1.38.1 (Schloss et al., 2009). Sequences were pre-processed following the standard operating procedure (MiSeq SOP) (Kozich et al., 2013). Pre-processed sequences, which were aligned and normalized, were used to generate an uncorrected pairwise distance matrix, which was then used to cluster the sequences using the furthest neighbour algorithm and to detect OTUs at a genetic distance of 0.03. OTUs detected at this distance were classified by comparing a representative sequence from each cluster against the SILVA-SEED (v138) reference database (Quast et al., 2013), using The Basic Local Alignment Search Tool (BLAST) to identify similar sequences (Altschul et al., 1990) and the k-Nearest Neighbour algorithm to determine the consensus taxonomy from the 10 most similar sequences in the database. Sequences were classified following the SILVA-SEED (v138) taxonomy scheme (Yilmaz et al., 2014) where the Genome Taxonomy Database (GTDB) (Parks et al., 2019). Chao 1 estimator and Shannon index were calculated to predict community richness using PAST software 50 (Hammer et al., 2001).

2.6. Statistical analysis

Principal Component Analyses (PCA) on the relative proportion of OTUs (at a 0.03 distance) among the samples were obtained. Using the three components as new variables, hierarchical dendrograms by Euclidean squared distance method were also calculated (IBM SPSS Statistics 23 package). Redundancy analysis (RDA) was performed by CANOCO 4.5 software (Microcomputer Power, Ithaca, NY, USA) (Braak and Šmilauer, 2002). Chao 1 estimator and Shannon diversity index of the individual domains, as well as the relative percentages of the identified OTUs (at a distance of 0.03) were utilized as biological datasets. As environmental variables, pH, ORP, T, DO, EC, turbidity, Chl-a, PC, PAR, SD, total N and total P were used. Data were transformed using ln(x + 0.1) and normalized to zero mean and unit variance. Graphical presentation was performed using CANODRAW 4.0 software. Although the RDA was calculated based on the relative percentage of all identified OTUs, the triplot only displays the OTUs that were detected in a proportion of >3 % at one of the sampling sites.

To elucidate the intricate relationships within microbial communities across various sampling points, a co-occurred network analysis was carried out. The network was constructed based on a Bray-Curtis dissimilarity index set at a threshold of 0.5, capturing the dissimilarities between community compositions. This index effectively represented the dissimilarity of communities. Additionally, the network incorporated nodes and edges representing the relative abundances of OTUs, with a stringent criterion of inclusion — only those OTUs surpassing an abundance threshold of 3 % were considered. The resulting network comprised 42 nodes and 105 edges, yielding an average degree of 8.2, which provided insights into the connectivity and complexity of the microbial interactions. Network construction and analysis were carried out utilizing the NetworkX package in the Python programming language.

PCA, RDA and networks are extensively employed in environmental scientific studies due to its capacity to simplify complex datasets into essential components, facilitating a more profound understanding of underlying patterns and relationships. These methodologies excels in

identifying the most significant sources of variation within datasets, thereby reducing the dimensionality and highlighting the dominant factors influencing environmental patterns. This reduction in dimensionality is crucial for simplifying complex environmental systems and uncovering key drivers of change (Zuur et al., 2007; Faust, 2021).

3. Results

3.1. Surface water contribution and wetland hydrochemistry

During this study, the Guadiana River (E2, G3, G6) and the Cigüela River (E1) inflows were active only in April (spring). The Guadiana River presented higher pH value (8.57) and less EC (1567 $\mu\text{S}/\text{cm}$) than the Cigüela River (pH 7.82 and EC 1706 $\mu\text{S}/\text{cm}$, Table 1). However, both inflows exhibited the same hydrochemistry, i.e. calcium sulphated waters with bicarbonate as the second dominant anion (Table 2S).

Precisely in spring, the wetland in Zone A presented calcium sulphated water, and in Zone B together with sample 2A calcium-magnesium sulphated water. Sample 2A, influenced by the Cigüela River (Fig. 1) showed similar values of chlorine and bicarbonate (Table 2S). In summer, all samples showed higher mineralization due to the usual evapoconcentration process. With respect to trace elements, the obtained concentrations showed low values (Table 2S).

As respect to the physico-chemical parameters, the wetland presented a circumneutral pH, showing homogeneous values in Zone B (pH 7.80) and heterogeneous values in Zone A (range 7.99–8.37 in spring, and 8.31–8.80 in summer). EC reflects the different degrees of mineralization of the two main contributions of water to the wetland, set at 2600 $\mu\text{S}/\text{cm}$ in the area of influence of the Cigüela River (sample 2A) and $\sim 1,800$ $\mu\text{S}/\text{cm}$ in the area of the Guadiana River (samples 1A, 4A, 7A, 9A). The vertical distribution of the physico-chemical parameters has a general tendency not to show important differences with depth (e.g. pH, T, EC, Chl-a), although there are some parameters that present changes. The redox potential showed a negative gradient with depth, reaching negative values in the wetland bottom, especially in summer. This indicates an anoxic medium. DO showed values slightly sub-saturated or with daily variations of the sub/over-saturation cycle in relation to the photosynthetic activity of phytoplankton.

Turbidity has always been present throughout the wetland, generally higher in Zone A (values between 11 and 14 NTU in spring, and 88–105

NTU in summer), than in Zone B (2–4 NTU in spring, and 3–10 NTU in summer). Turbidity, Chl-a and PC average values in summer are higher than in spring in both zones (Table 1).

Regarding nutrients, water samples from the wetland presented TN and TP contents ranging between 2.16 and 13.40 mg/L and 0.01–0.18 mg/L, respectively (Table 1), showing a strong increase of both nutrients in summer, especially in Zone A.

TN measured in the Cigüela River was low (1.68 mg/L), and TP was high (0.70 mg/L) when compared to the values obtained of the Guadiana River (0.04 mg/L TP and 4.81 mg/L TN) (Table 1).

3.2. Wetland trophic state

Criteria for trophic status classification using chlorophyll-a (Chl-a), total phosphorus (TP) and transparency, using Secchi disk (SD), as water quality parameters (OECD, 1982) are given in Table 1Sa. Concerning the SD values, these data cannot be directly applied in our case study, due to the shallow nature of the wetland, with maximum depths of two meters (Table 1), leading to an error in classification. Therefore, in addition to the OECD classification standards, we here considered the measurement of light penetration at the wetland bottom as a valuable parameter to evaluate the trophic state of shallow-water wetlands, instead of transparency with SD. This evaluation aims to ascertain the minimum levels of Photosynthetically Active Radiation (PAR) reaching the bottom of the wetland, at which benthic vegetation grow (Fig. 2b).

The PAR threshold for benthic vegetation growth in the TNBP wetland was determined by choosing the lowest PAR values observed during summer at sampling sites with charophytes (12S and 15S), with a designated range of 20–40 $\mu\text{mol}/\text{sm}^2$ (Table 1). Hence, under the standards chosen to be used in our study case, Zone A of the wetland was considered eutrophic in spring and hypereutrophic in summer, while Zone B was considered eutrophic in both seasons (Table 1Sb).

3.3. Sequencing analysis and estimated richness

The collection of amplicons was sequenced, and the number of reads is summarized in Table 3S. A total of $\sim 4.5 \times 10^6$ sequences – both 16S rRNA and 18S rRNA genes – were obtained across all samples, about 146,000 per sample on average. The analysis of the read length distributions indicated a modal distribution between 442 and 444 nucleotides

Table 1

Field parameters and nutrients of inputs and sampling sites in the wetland measured during spring (April-18) and summer (September-18). M Depth: Maximum depth. SD: Secchi disk. *: Not analysed. Values of field parameters are the mean of the water column. ORP values are the mean of the water column, removing values from the wetland bottom.

	Sample	M Depth	T	DO	EC	pH	ORP	Turb	PC	Chl-a	total N	total P	SD	PAR (M Depth)		
														m	$^{\circ}\text{C}$	mg/L
April-18	Inflows	E1	*	20.2	9.16	1,706	7.82	215	13	0.18	3.85	1.68	0.67	*	*	*
		E2	*	17.6	8.57	1,567	8.57	61	17	0.38	6.45	4.81	0.04	*	*	*
		G3	1.29	17.2	6.30	1,370	7.28	204	32	0.24	4.14	8.70	0.04	44	97	*
		G6	*	23.0	8.64	1,330	7.85	167	4	0.13	4.40	8.21	0.03	*	*	*
	Zone A	1A	1.23	15.4	8.26	1,774	8.22	124	14	1.07	13.34	3.92	0.08	53	16	0.40
		2A	0.73	15.1	7.74	2,617	7.99	107	11	1.53	17.06	2.73	0.08	52	53	1.73
		4A	1.04	15.4	8.64	1,851	8.30	96	12	1.40	15.97	2.43	0.06	56	5	0.08
		7A	2.00	15.5	8.23	1,871	8.37	144	13	1.40	17.71	2.16	0.05	61	2	0.05
		9A	1.20	15.3	8.20	1,910	8.32	160	11	1.51	17.46	2.28	0.05	76	33	1.02
		11A	1.92	17.1	9.28	2,531	7.82	105	4	0.73	13.12	2.78	0.06	132	19	0.41
		12A	1.42	16.9	9.57	2,756	7.89	98	3	0.54	12.44	2.56	0.04	142	200	4.48
Zone B	15A	1.55	17.0	8.76	2,806	7.79	103	2	0.57	9.78	2.49	0.04	155	272	6.39	
	17A	1.80	16.9	8.97	2,839	7.85	140	2	0.47	11.88	2.80	0.04	148	45	1.16	
	1S	0.89	22.9	5.43	3,047	8.32	149	105	19.73	31.92	10.40	0.17	11	15	0.36	
	4S	0.51	23.2	5.44	3,103	8.30	167	97	19.52	31.27	13.40	0.18	12	3	0.07	
	7S	1.83	22.9	5.28	3,100	8.30	43	88	19.37	34.34	10.20	0.16	10	0	0	
September-18	Zone A	9S	0.44	24.9	5.18	3,094	8.82	89	88	18.08	32.07	10.20	0.18	11	0	0
		12S	1.81	24.2	6.62	3,454	7.95	131	10	2.15	23.40	3.30	0.07	56	42	1.05
		13S	1.94	24.2	6.42	3,479	7.88	153	7	1.84	21.82	4.22	0.06	65	19	0.51
		15S	1.48	26.4	7.26	3,463	7.66	184	3	0.77	15.51	2.70	0.05	85	22	0.71
		17S	2.40	26.2	7.56	3,462	7.81	200	3	0.58	13.55	5.07	0.05	101	56	1.43

(nt). After quality control checks, chimera sequence removal and controls sequences subtraction, a total of $\sim 1.9 \times 10^6$ sequences remained, corresponding around 102,000 per sample to Bacteria, 76,000 to Eukarya, and 700 to Archaea. The number of OTUs detected at a distance of 0.03, was ca. 500 per sample in Bacteria, 90 in Eukarya, and 13 in Archaea, with a total of 6944 of OTUs detected. Nevertheless, Chao1 estimations suggest that we were able to identify from 78 to 100 % of the total OTU population. In general, samples taken during spring showed higher number of OTUs than the summer ones (~ 25 % less in Bacteria and Eukarya, and 60 % less in Archaea). Shannon diversity index was higher for Bacteria and Eukarya (3.7 and 2.7, respectively) than in case of Archaea (1.8).

3.4. Taxonomic composition and diversity of the bacterial community

A total of $\sim 1.2 \times 10^6$ sequences were clustered and classified into 5635 target Bacteria OTUs (Table 3S). The lowest number of target reads and OTUs were recorded for all sites in summer ($\sim 88,000$ sequences and 381 OTUs on average). In contrast, in spring, the average number of reads and OTUs were higher in all sampling sites ($\sim 112,000$ sequences and 561 bacterial OTUs), except for site 7A, which showed the lowest values ($\sim 56,000$ sequences). The highest number of bacterial OTUs were found in the Guadiana River sampling sites (G3A and G6A) as well as in the entrance of the park (E2A) with 654 OTUs on average. The bacterial community diversity showed a similar pattern in both sampling seasons, with the highest Shannon diversity recorded in the Guadiana River samples (G3A = 4.84 and G6A = 4.26).

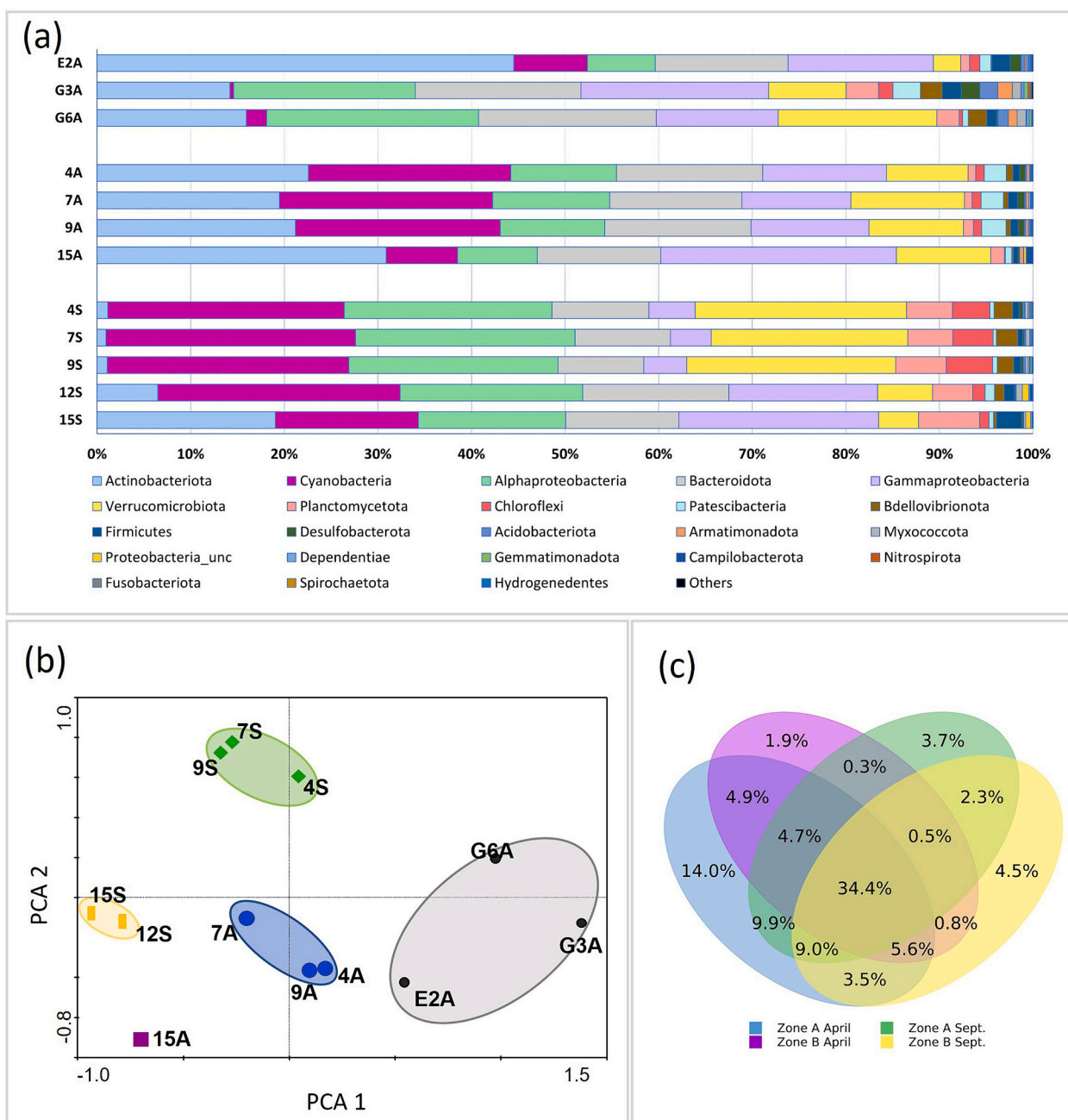


Fig. 3. Relative abundance of bacterial OTUs. a Histogram showing relative abundance of major bacterial phyla-class level per sampling site and sampling date. b Principal Component Analyses (PCA) on the relative proportion of bacterial phyla-class level. Ellipses represent the different populations detected in terms of phylogenetic community composition and relative abundance. c Venn diagram at distance of 0.03 of the shared OTUs among sampling zones and sampling date.

Altogether, 41 bacterial phyla/classes were detected (Fig. 3a). The most abundant bacteria were affiliated with the Actinobacteriota (being up to 44 % in E2A), Cyanobacteria (~20 % in all sampling sites except E2A, G3A and G6A), Alphaproteobacteria, Bacteroidota and Gammaproteobacteria (~15 % in most sampling sites), and Verrucomicrobiota (~10 % in most sampling sites). These groups represented 80 %–90 % of the total bacterial microbial community. Additionally, clear differences in the bacterial seasonal distribution were found in all samples, being more evident in Zone A than in Zone B. Actinobacteriota and

Gammaproteobacteria were highly reduced in summer (from ~22 % and ~13 % respectively in spring to <3 % in summer for sampling sites 4, 7 and 9). Alphaproteobacteria and Verrucomicrobiota increased their percentages in summer, i.e. ~10 % for both phyla in spring and ~22 % in summer from sampling sites inside the park. Verrucomicrobiota did not increase their percentages in samples 12S and 15S (Fig. 3a and Fig. 1S).

With the PCA on the relative proportion of bacterial OTUs (at a 0.03 distance), 93 % of the total variance was explained. This analysis

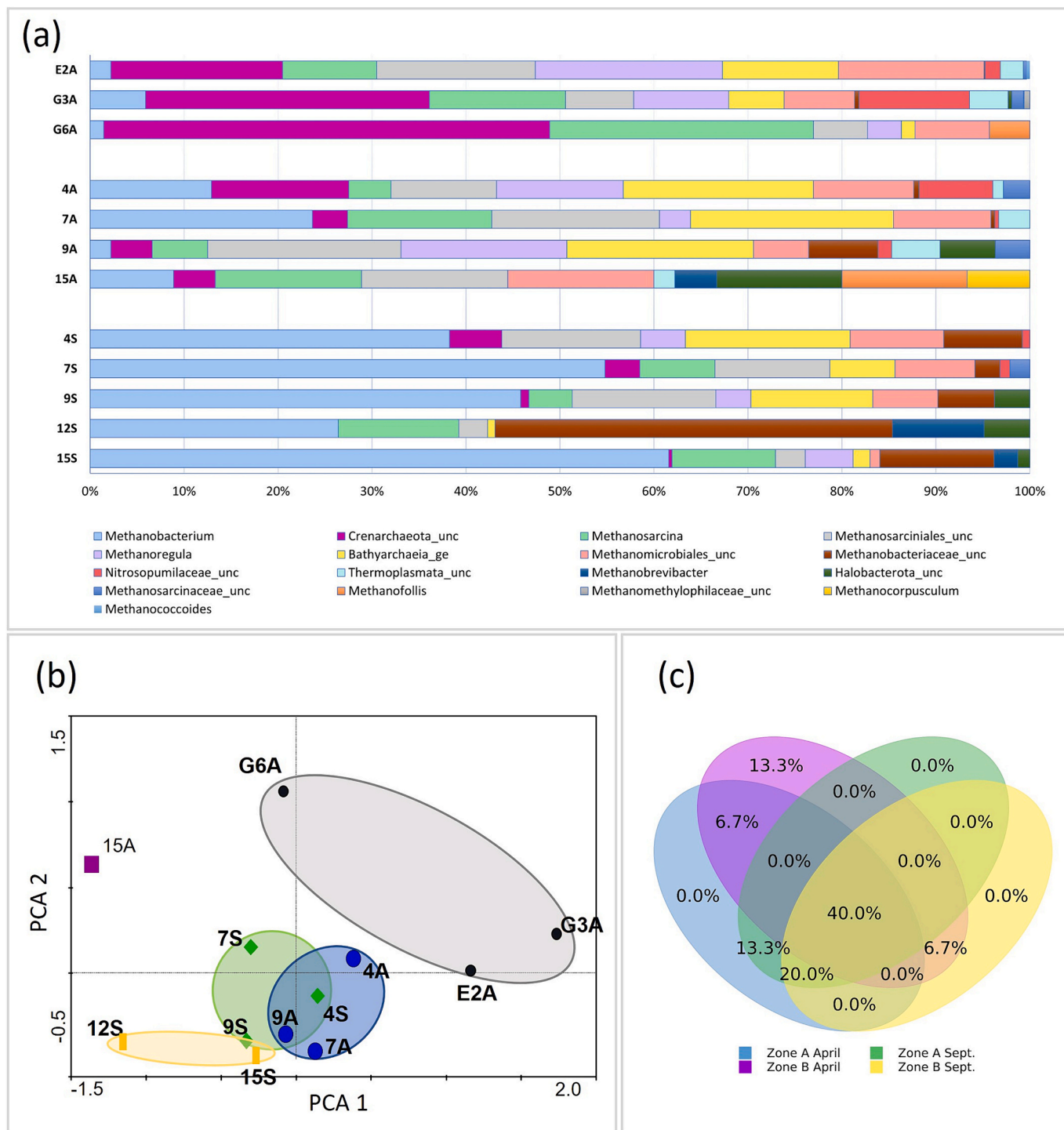


Fig. 4. Relative abundance of archaeal OTUs. a Histogram showing relative abundance of major archaeal genera level per sampling site and sampling date. b Principal Component Analyses (PCA) on the relative proportion of archaeal genera level. Ellipses represent the different populations detected in terms of phylogenetic community composition and relative abundance. c Venn diagram at distance of 0.03 of the shared OTUs among sampling zones and sampling date.

showed a bacterial composition with a clear geographical and seasonal distribution, grouping into four different clusters: (i) samples from Guadiana River (G3A and G6A), (ii) samples from Zone A collected in spring (4A, 9A, 7A) as well as the nearby entrance sample (E2A), (iii) samples taken in Zone A during summer (4S, 9S, 7S), and (iv) samples from Zone B (12A, 15S) (Fig. 3b). The bacterial community shared only 34.4 % of the target bacterial OTUs between samples, showing a high contribution (14 %) of unique OTUs in Zone A samples collected in spring (Fig. 3c).

3.5. Taxonomic composition and diversity of the archaeal community

Regarding the archaeal community, a total of $\sim 8 \times 10^3$ sequences were clustered and classified into only 157 target Archaea OTUs (Table 3S). In this case, the lowest number of target reads and OTUs were also found for all sites in summer (~ 600 sequences and 10 OTUs on average), when compared to spring samples (~ 800 sequences and 15 OTUs). The archaeal community diversity also showed a similar pattern in both sampling seasons, with the lowest Shannon diversity recorded in the Zone B samples (12S = 1.34 and 15S = 1.2). Furthermore, 17 genera were detected (Fig. 4a).

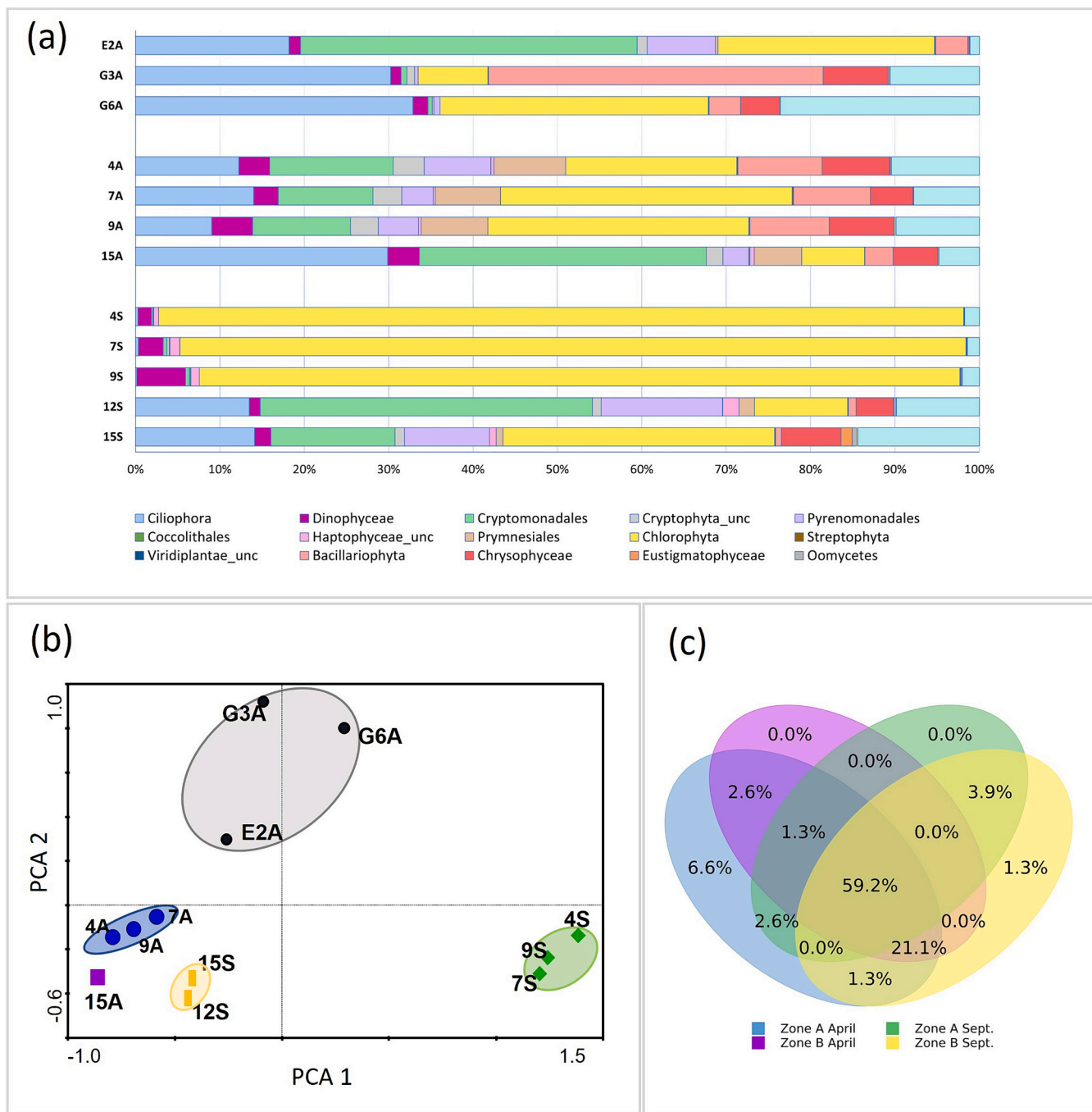


Fig. 5. Relative abundance of eukaryotic OTUs. **a** Histogram showing relative abundance of major eukaryotic phyla-class level per sampling site and sampling date. **b** Principal Component Analyses (PCA) on the relative proportion of eukaryotic phyla-class level. Ellipses represent the different populations detected in terms of phylogenetic community composition and relative abundance. **c** Venn diagram at distance of 0.03 of the shared OTUs among sampling zones and sampling date.

The most abundant groups were *Methanobacterium*, Crenarchaeota and Methanosarcinales (including *Methanosarcina*), comprising up to 50 % of the total number of archaeal sequences. Around 70 % of all archaeal sequences were affiliated to taxa related to methane metabolism. Clear seasonal differences were also found in samples 4, 7, 9 and 15. *Methanobacterium* and related uncultured *Methanobacteriaceae* increased in summer (from ~14 % to 2 % in spring respectively, up to 50 % and 15 % respectively in summer). Besides, Crenarchaeota were highly represented in the entrance and in Guadiana River samples (E2A, G3A, G6A), being ~30 % of the total sequences (Fig. 4a and Fig. 1S).

PCA on the relative proportion of archaeal OTUs (at a 0.03 distance) explained 82 % of the total variance. In general, archaeal community showed also a clear geographical and seasonal distribution, grouping in three main clusters (Fig. 4b): (i) samples from the Guadiana River (G3A) and E2A, (ii) samples from Zone A collected in spring (4A, 7A, 9A) and summer (4S, 7S, 9S, 15S), and (iii) samples taken in Zone B during summer (12S, 15S). The archaeal community shared 40 % of the target OTUs between all samples, showing the higher contribution (13 %) of unique OTUs in Zone B samples collected in spring (Fig. 4c).

3.6. Taxonomic composition and diversity of the eukaryotic community

Regarding the eukaryotic community, a total of $\sim 1 \times 10^6$ sequences were clustered and classified into 1152 target Eukarya OTUs (Table 3S). The lowest number of reads and OTUs were again found in summer for most of the sampling sites ($\sim 5 \times 10^4$ sequences and 80 OTUs on average) when compared to spring ($\sim 9 \times 10^4$ sequences and 109 OTUs). In this case, the eukaryotic community showed higher diversity in spring (averaged $H = 3$) than in summer (averaged $H = 2.3$), with the lowest Shannon index recorded in Zone A for summer samples.

Most of the Eukarya were distributed among the phyla/class *Chlorophyta* (32 % of the total eukaryotic sequences), *Cryptomonadales* (18 %), *Ciliophora* (16 %), *Stramenopiles*, *Bacillariophyta* and *Pyrenomonadales* (22 %), which made up ≥ 90 % of the total Eukarya within each sampling site (Fig. 5a). *Chlorophyta* was the most relative abundant group in most of the sampling sites, except for 12S, 15A and E2A where *Cryptomonadales* were predominant. Within *Chlorophyta*, the genus *Hydrodictyon* represented >30 % of the total reads in whole the zone. Other *Chlorophyta* highly represented were *Scenedesmaceae* (13 % of the *Viridiplantae* sequences), *Sphaeropleales* (11 %) and the genus *Oocystis* (9 %) (Fig. 1S).

Within the *Cryptomonadales*, the genera *Cryptomonas*, *Teleaux* and *Hanusia* were the most abundant, being up to 40 % of the *Cryptomonadales* sequences. Ciliates were also frequently found in all samples, except in the case of Zone A sampling sites in summer (4S, 7S and 9S). In this case, *Halteria* and species belonging to the *Intramacronucleata* subphylum were the most abundant taxa, representing up to 50 % of the total *Alveolate* sequences.

Finally, *Bacillariophyta* species were mainly found in all sampling sites in spring. *Navicula* and *Skeletonema* were the most abundant genera, representing >50 % of the total *Bacillariophyta* sequences. In this case, PCA explained 86 % of the total variance (Fig. 5b) and it showed also a clear geographical and seasonal distribution, grouping in four different clusters, as well as in the case of prokaryotes, although with minor differences: (i) the inflow samples collected in spring (E2A, G3A, G6A), (ii) samples from Zone A collected in spring (4A, 7A, 9A), (iii) samples taken in Zone A during summer (4S, 7S, 9S), and (iv) samples collected in Zone B during summer (12S, 15S). The eukaryotic community shared ~60 % of the target OTUs between all samples, showing the highest contribution (~7 %) of unique OTUs in Zone A samples collected in spring (Fig. 5c).

3.7. Correlation between microbial community composition and environmental parameters

Redundancy analyses (RDA) of 16S/18S rRNA gene amplicons data sets were applied to correlate the measured environmental parameters

and microbial community structure and were illustrated in triplots, where taxa names are represented in blue and physico-chemical parameters in black (Fig. 6). The eigenvalues for each axis generated by RDA indicate how much of the variation seen in species data can be explained by that canonical axis. In this case, 80 % of the correlation between OTUs, sampling sites and environmental data was explained by two axes (56.9 % axis 1, 80.1 % axis 2). The significance test of the first canonical axis yielded a p value <0.05 .

Axis 1 (vertical axis) showed positive correlations across numerous environmental indicators, i.e. Total N, PC, Chl-a, EC, T, pH, and turbidity. Conversely, it exhibited negative correlation to ORP, SD, DO, and Bacteria and Eukarya Shannon indexes (red and green arrows, respectively). Sampling sites 4S, 7S and 9S clustered together and were positively correlated to a high number of environmental parameters, as well as to *Terrimicrobiaceae* (*Fuku*), Rhizobiales (A0839), *Chthoniobacteriaceae* and Cyanobacteria, and to *Hydrodictyon*, *Tetrachlorella*, *Chlorella* and Spharo Eukarya lineages, but negatively correlated to rest of Bacteria and Eukarya. By contrast, no archaeal lineage is clearly associated with this cluster and conditions. 12S and 15S samples were most clearly discriminated by Axis 2 (horizontal axis). Both correlated positively to EC and T and negatively to Archaea Shannon index. These samples are correlated clearly to *Tolypothrix* and Bacteroidetes bacteria and *Cryptomonadaceae* Eukarya lineage (Fig. 6).

Samples from spring resulted in a positive correlation between them and ORP, SD, DO concentration and Bacteria and Eukarya Shannon indexes, some bacterial lineages such as *Limnobacter* and *Cyanobium*, some eukaryotic lineages such as *Oocystis* and *Navicula*, and most methanogenic archaea. It is interesting to note that spring samples are grouped together, but also separated by zones.

3.8. Microbial network in sampling sites

Within the resulting network, nodes representing the sampling sites are displayed in 4 clusters (Fig. 7): (i) 4A, 7A, 9A 15A and E2A central cluster, which presents high numbers of connections to taxonomic nodes; (ii) G3A and G6A Guadiana River cluster; (iii) 4S, 7S and 9S cluster; and (iv) 12S and 15S cluster. Some nodes classified as Bacteria and Eukarya lineage are cluster-specific. Thus, *Microbacteriaceae*, *Tolypothrix*, *Hanusia* and *Sphaeropleales* are only connected to 12S and 15S cluster; *Limnhabitans*, *hgcl_clade*, *Navicula* and *Cryptomonas* are connected to central cluster; and *Bacillariophyta*, *Intramacronucleata* and *Pseudictyospharium* are exclusively connected to the Guadiana River cluster. Nodes classified as Cyanobacteria, *Scenedesmaceae* and *Hydrodictyon* appear only in 4S, 7S and 9S cluster.

By contrast, most of the nodes classified as Archaea present connections to different clusters. For example, *Methanobacterium* is connected to all clusters except for the Guadiana River cluster. Methanosarcinales and *Bathyarchaeia* nodes are connecting central cluster and 4S, 7S and 9S cluster. Methanosarcina and Methanoregula nodes also connect three clusters except for 4S, 7S and 9S cluster. It is interesting to note that neither Bacteria nor Archaea domains are specific of the Guadiana River cluster. The central cluster (spring samples and input sample) has the highest number of connected and shared nodes.

4. Discussion

4.1. Seasonal environmental and microbiological characteristics of the TDNP wetland

TDNP wetland experiences pronounced seasonal fluctuations, influenced by its location in an arid climate with warm to hot temperatures and irregular to scarce rainfall. Additionally, the wetland's reduced depth and the anthropic actions further heighten its sensitivity to these seasonal changes (Ortiz-Jiménez et al., 2006). As a result, TDNP wetland becomes susceptible to eutrophication, and standard physico-chemical

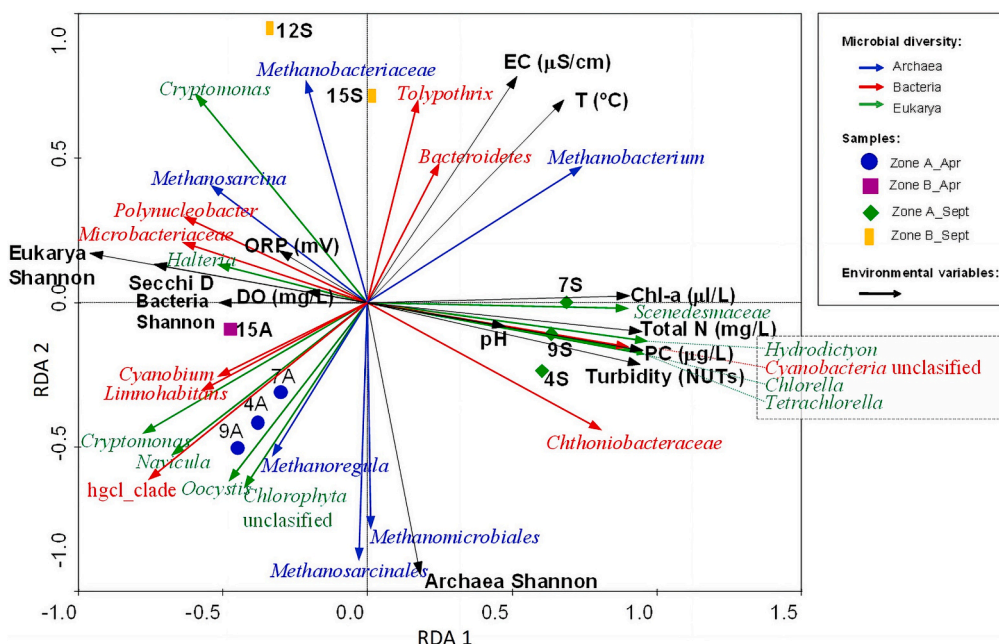


Fig. 6. Redundancy correspondence analysis (RDA) triplot. 89.6 % of the correlation between relative abundance of OTUs, samples sites and environmental data was explained by two axes. Biological variables were compound by Shannon indexes; Environmental variable were represented by conductivity (EC), temperature (T), chlorophyll-a (Chl-a), total nitrogen (Total N), phycocyanin (PC), turbidity, pH, oxygen concentration (DO), Secchi disk (Secchi D), and redox potential (ORP).

values of T, EC, pH and nutrient availability characteristic of semi-arid aquatic systems are affected. Moreover, the effects of these seasonal changes differ between zones A and B, with a stronger impact on Zone A due to its shallower depth, the absence of benthic vegetation (*Chara* spp.), and the presence of fish that stir up the sediment, affecting the water column (Fig. 2d).

During spring (April), when water levels are high owing to inflows from the Cigüela and Guadiana rivers, both wetland zones can be characterized as eutrophic (Table 1Sb), presenting certain transparency in the water column that allows light to reach the bottom of the wetland (Table 1). Macrophytes were identified around sampling sites (15A), where PAR values (up to 272 $\mu\text{mol}/\text{sm}^2$) were measured (Fig. 2b). Previous studies (Schwarz and Hawes, 1997; Vieira and Necchi, 2003; Wang et al., 2015) present a wide range of PAR values in which macrophytes can develop.

Regarding hydrochemical characterization, the Cigüela River contributes brackish waters with elevated mineralization levels, originated from the watershed's evaporitic materials (EC 1706 $\mu\text{S}/\text{cm}$; Table 1), and enriched in Na^{2+} , K^{+} , Mg^{2+} , SO_4^{-} , and Cl^{-} (Table 2S). The blending of these brackish waters with lower mineralization and sulphate levels from the Guadiana River defines the uniqueness of this wetland (Berzas et al., 2000).

In summer (September), the inactivation of the inflows, the irregular to absence rainfall, the water level reductions (especially in Zone A), the high temperatures, and the evaporation-induced evapoconcentration, lead to the disruption of the wetland's water quality. This is translated in an increase of dissolved solids (>EC) and substantial changes in physico-chemical parameters, i.e. lower transparency (SD) and higher turbidity, Chl-a, PC, and nutrients (TP and TN) (Table 1). The alterations in Zone A during the summer are more pronounced, elevating the trophic status to hypertrophic, while Zone B remains eutrophic (Table 1Sb), with some areas even experiencing macrophyte growth (Fig. 2b), where PAR values were up to 56 $\mu\text{mol}/\text{sm}^2$. Moreover, considering that eutrophic waters are typically deemed of poor quality and the presence of macrophytes is indicative of good water quality (Maggioli et al., 2009), the occurrence of macrophytes in semi-arid shallow-water wetlands could be considered as an additional parameter for assessing their trophic status.

The microbial diversity detected in the TDNP wetland is similar to other wetlands (Lirós et al., 2014; Newton et al., 2011; Wang et al., 2022). The most abundant microorganisms were bacteria — a total of $\sim 1.2 \times 10^6$ sequences, followed by Eukarya with $\sim 1 \times 10^6$ — affiliated to Actinobacteriota, Cyanobacteria, Bacteroidota, Alphaproteobacteria, Gammaproteobacteria and Verrucomicrobiota. These groups represented ~ 90 % of the total bacterial microbial community. Most of the Eukarya were distributed among the phyla/class *Chlorophyta* (32 % of the total eukaryotic sequences), *Cryptomonadales* (18 %), *Ciliophora* (16 %), *Stramenopiles*, *Bacillariophyta* and *Pyrenomonadales* (22 %). Concerning Archaea, around 70 % of the sequences were affiliated to species related to methane metabolism, mainly *Methanobacterium* sp., and within *Methanosarcinales* order (Figs. 3–5).

In general, samples taken during spring showed higher number of OTUs than the summer ones (~ 25 % less in Bacteria and Eukarya, and 60 % in Archaea) (Table 3S). This indicates that microbial community diversity tended to be higher in waters with lesser eutrophication, as also reported by Feng et al. (2019), and Wang et al. (2022, 2023).

4.2. Impacts of hypereutrophication and phytoplankton bloom in the microbial community

A strong water level reduction is an important driving factor of phytoplankton dynamics, suggesting that it alters the light and mixing regime, and increases nutrient concentrations and phytoplankton biomass favouring phytoplankton blooms (Costa, 2016). In summer, a green superficial layer was observed in Zone A accompanied by an increase in turbidity (80–120 NTU), nutrients (up to 13.40 mg/L TN and 0.18 mg/L TP) and high concentrations of Chl-a (up to 40 $\mu\text{g}/\text{L}$) and PC (~ 20 $\mu\text{g}/\text{L}$), indicating a shift in the trophic status from eutrophic to hypereutrophic (Table 1Sb). Chl-a and PC values indicate the development of a phytoplankton bloom, since these parameters can be used as a proxy for biomass of algae and cyanobacteria, respectively (Rousso et al., 2021). The rise of PC coincides with the increase of *Tolypothrix* (nitrogen-fixing filamentous cyanobacteria) and unclassified Cyanobacteria, displacing *Cyanobium* (nitrogen non-fixing unicellular cyanobacteria; Fig. 1S, Figs. 6 and 7). Likewise, the strong increase in Chl-a

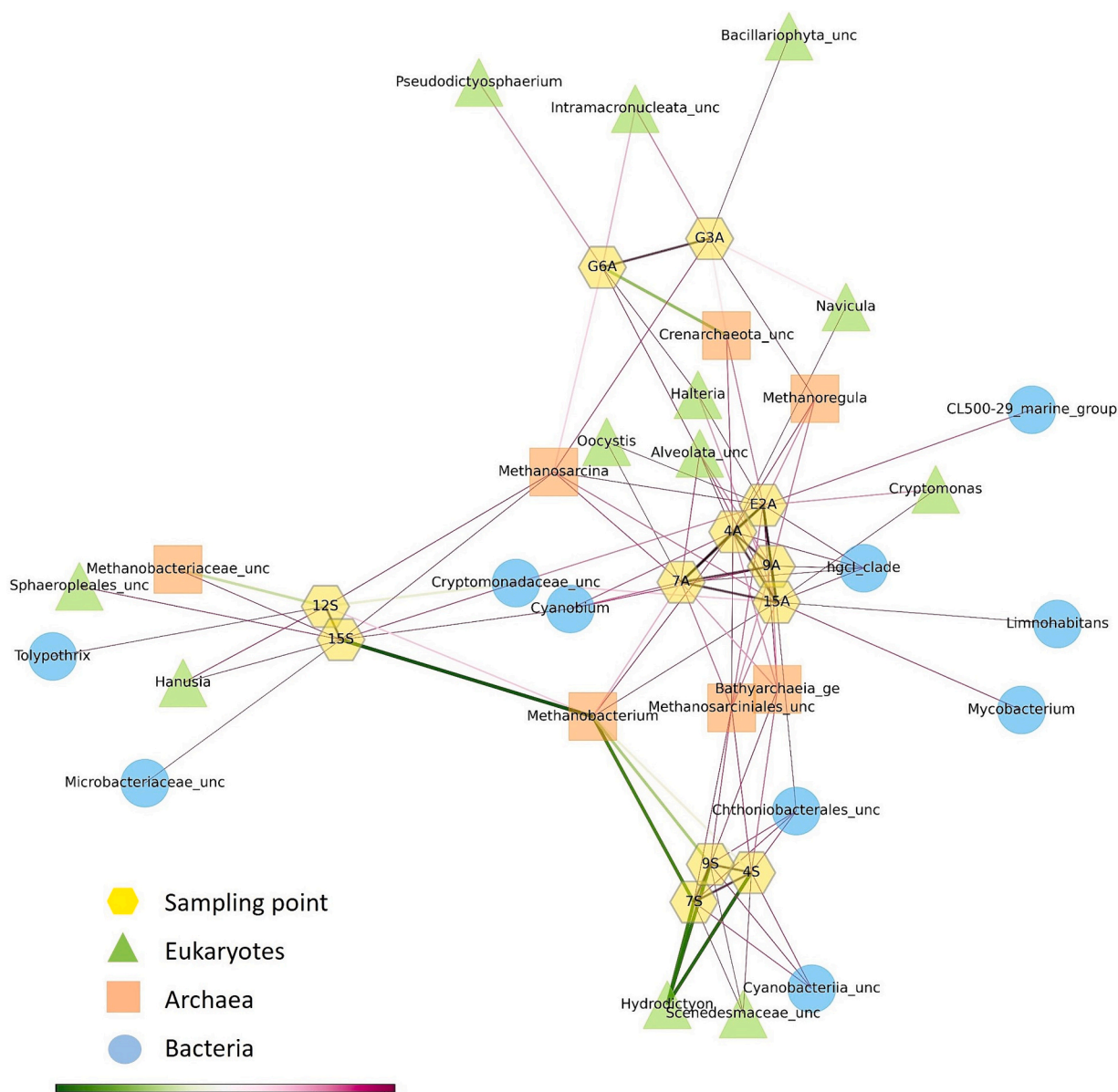


Fig. 7. Microbial correlation network. Bacterial, archaeal and eukaryotic OTUs with relative abundance >3 % in any of the samples were assigned to the genus level and represented as nodes in the network. Correlation network between the different sampling sites. The network was calculated with Bray-Curtis dissimilarity (BC) bounded between 0 and 1. The knowledge network was calculated by setting BC to 0.5 and 42 nodes and 106 edges with a mean degree of 8.2 were obtained.

values coincides with the clear bloom of chlorophytes, especially *Hydrodictyon*, although an increase of other taxa of this phylum (*Scenedesmaceae*, *Sphaeropleales*, *Tetrachlorella* and *Chlorella*) was also observed (Fig. 1S and Fig. 6). *Hydrodictyon* algae are therefore the principal responsible of the bloom.

The *Hydrodictyon* bloom (organic suspended solids) coupled with the shift from non-nitrogen fixing to nitrogen-fixing cyanobacteria (Fig. 6) caused the rise in turbidity and nutrients (TP and TN). This led to a drop in values of light penetration ($0\text{--}15\ \mu\text{mol}/\text{sm}^2$) impacting water transparency and hindering charophyte growth. Thus, primary production cannot exist in depth, promoting the lack of DO in the water column (Table 1) (Tas, 2011), enhanced by consumption of oxygen and the degradation of organic matter (Xiaoran et al., 2013). These changes explain the significant negative correlation between the samples of Zone A with eukaryotic community diversity (and abundance) and DO observed in the RDA plot (Fig. 6). Furthermore, there is a positive correlation between pH and eukaryotic photosynthetic bloom-related taxa,

as an increase of pH is more conducive to increase plankton reproduction (Li et al., 2022; Wang et al., 2016).

A change in heterotrophic microbial populations is also detected as a consequence of the algal bloom, like the displacement of Actinobacteriota. This phylum, typically serving as a microbial indicator for healthy wetlands with low nutrient and pollution levels (Newton et al., 2011; Urakawa and Bernhard, 2017), has been noted to experience a decrease in abundance in eutrophic wetlands (Wang et al., 2023). Opposite is the case for Verrucomicrobiota, whose representatives (Chthoniobacteriales and FukuN18) are clearly increased in summer (Fig. 3). Verrucomicrobiota has been previously detected in TDNP by D'Auria et al. (2010) who reported the ability of some species to ferment a variety of sugars (aerobic or facultative chemoheterotrophs), which explain their increase with higher values of turbidity, TN, TP and TOC (Table 1 and Table 2S). Additionally, keystone taxa of Chthoniobacteriales (Verrucomicrobiota), Bacteroidota or Rhizobiales are known to adapt to environments of high organic complexity.

The increase in nitrogen deposition, linked to an increase of phytoplankton biomass (Duce et al., 2008), generates a loss of biodiversity (Bobbink et al., 2010) and higher susceptibility to stress factors in communities (Pardo et al., 2011). Our results support the loss of biodiversity since samples taken in spring have higher number of OTUs and Shannon index than in summer for Bacteria, Archaea and Eukarya. In Zone A, protists practically disappear at the time of the *Hydrodictyon* bloom, and Shannon index decreases more (from 3.2 to 2) than the other two domains (Table 3S). In the case of Archaea, the number of OTUs and diversity indexes were in general very low, which indicates the reduced role in the wetland waters, in line with other wetlands studies (Horton et al., 2019). Most of the archaea detected were classified as methanogenic, organisms commonly found in freshwater sediments and wetlands (Horton et al., 2019; Li et al., 2020a, 2020b). The increase in summer of methanogens (mainly Methanobacteriales) corresponds with an increase in turbidity (inorganic suspended solids), organic matter and a strong drop of DO, addressing a disturbance and movement of the sediments into the water column, favoured by fish activity (Fig. 2c) and wind associated to the reduction of the water depth (de Carvalho et al., 2017; Laguna et al., 2016).

An algal bloom like the one observed in TDNP entails a general loss in population and biodiversity of Bacteria, Eukarya and Archaea. In spring, a healthy wetland system in an environment dominated by a diversity of producers and decomposers; in summer with the algal bloom, to one that basically consists on primary producers and with very low microbial diversity. Moreover, microbial community of the wetland clearly differs from the communities in the inflows (Figs. 3–5), supporting a specific adaptation to this niche (Fig. 7).

5. Conclusions

TDNP semi-arid wetland undergoes strong season variations affecting its physico-chemical parameters, mainly due to its geographical situation, shallow water depth and anthropic actions.

Microbial community composition shows a clear geographical and seasonal distribution within the wetland as response to changes in the trophic status of the wetland, regulating the inter-domain microbial adaptation. During the spring, when the wetland exhibits optimal water quality (eutrophic), all samples of the wetland, including the entrance to the Guadiana River, display a similar microbial composition, resembling that of other freshwater wetlands. Conversely, samples obtained from the Guadiana River at its source and an intermediate point reveal differences, highlighting a distinctly diverse microbiology.

During the summer, the hypereutrophic zone shows significant alterations in both biotic and abiotic parameters of the wetland water. These changes create favourable conditions for the proliferation of algal bloom. The fluctuation of nutrient imbalances, especially concerning nitrogen sources, is the determining variable of planktonic network complexity and influences the diverse functions of keystone taxa. This results in a shift in the microbial community composition and a reduction in microbial abundance. Although eutrophic zone suffers minor variations in the water physical-chemical parameters, it also generates a response in microbial composition.

We propose to assess the photosynthetically active radiation (PAR) reaching the bottom of the wetland as an environmental parameter to determine water quality and therefore the trophic status of semi-arid shallow-water wetlands like TDNP.

Supplementary data to this article can be found online at <https://doi.org/10.1016/j.scitotenv.2024.171626>.

CRediT authorship contribution statement

Esther Santofimia: Writing – original draft, Validation, Supervision, Project administration, Investigation, Funding acquisition, Formal analysis, Conceptualization. **Elena González-Toril:** Writing – original draft, Validation, Supervision, Investigation, Data curation. **Graciela de**

Diego: Writing – original draft, Software, Formal analysis. **Blanca Rincón-Tomás:** Writing – original draft, Validation, Supervision. **Ángeles Aguilera:** Writing – original draft, Validation, Supervision, Investigation, Funding acquisition.

Declaration of competing interest

The authors declare no competing interests.

Data availability

Data will be made available on request.

Acknowledgements

The authors wish to thank the assistance and logistical support provided by the Conservation Director of the National Park, its environmental agents and support personnel, whose invaluable collaboration made sampling on the inundated surface of the park possible. We also want to thank Enrique López Pamo for his help in the development of this project.

Funding

This research has been funded by grants No. RTI2018-094867-B-I00 and PID2019-104205GB-C22 by the Spanish Ministry of Science and Innovation/State Agency of Research MCIN/AEI/10.13039/501100011033 and by “ERDF A way of making Europe”, as well as with funds from Fundación Biodiversidad (Ministry of Agriculture, Food and Environment Spain), Instituto Geológico y Minero de España and Next Generation EU-MINECRITICAL (C17.I7, MET2021-00-000).

References

- Aguilera, H., Castaño, S., Moreno, L., Jiménez-Hernández, M.E., de la Losa, A., 2013. Model of hydrological behaviour of the anthropized semiarid wetland of Las Tablas de Daimiel National Park (Spain) based on surface water-groundwater interactions. *Hydrogeol. J.* 21, 623–641. <https://doi.org/10.1007/s10040-012-0950-3>.
- Altschul, S.F., Gish, W., Miller, W., Myers, E.W., Lipman, D.J., 1990. Basic local alignment search tool. *J. Mol. Biol.* 215, 403–410. [https://doi.org/10.1016/S0022-2836\(05\)80360-2](https://doi.org/10.1016/S0022-2836(05)80360-2).
- Berzas, J.J., García, L.F., Rodríguez, R.C., Martín-Alvarez, P.J., 2000. Evolution of the water quality of a managed natural wetland: Tablas de Daimiel National Park (Spain). *Water Res.* 34, 3161–3170. [https://doi.org/10.1016/S0043-1354\(00\)00069-5](https://doi.org/10.1016/S0043-1354(00)00069-5).
- Bobbink, R., Hicks, K., Galloway, J., Spranger, T., Alkemade, R., Ashmore, M., Bustamante, M., Ciederby, S., Davidson, E., Dentener, F., Emmett, B., Erisman, J.W., Fenn, M., Gilliam, F., Nordin, A., Pardo, L., De Vries, W., 2010. Global assessment of nitrogen deposition effects on terrestrial plant diversity: a synthesis. *Ecol. Appl.* 20, 30–59. <https://doi.org/10.1890/08-1140.1>.
- Braak, C.J.F., Šmilauer, P., 2002. *CANOCO Reference Manual and CanoDraw for Windows user's Guide. Software for Canonical Community Ordination (Version 4.5)*. Microcomputer Power, Ithaca, NY 500.
- Bradley, I.M., Pinto, A.J., Guest, J.S., 2016. Design and evaluation of illumina MiSeq-compatible, 18S rRNA gene-specific primers for improved characterization of mixed phototrophic communities. *Appl. Environ. Microbiol.* 82 <https://doi.org/10.1128/AEM.01630-16>.
- Bravo-Martín, S., Mejías, M., García-Navarro, F.J., Jiménez-Ballesta, R., 2019. Current status of Las Tablas de Daimiel National Park Wetland and actions required for conservation. *Environments* 2019, Vol. 6, page 75 6, 75. doi:<https://doi.org/10.3390/ENVIRONMENTS6060075>.
- Carlson, R.E., 1977. A trophic state index for lakes. *Limnol. Oceanogr.* 22, 361–369. <https://doi.org/10.4319/LO.1977.22.2.0361>.
- Chao, C., Wang, L., Li, Y., Yan, Z., Liu, H., Yu, D., Liu, C., 2021. Response of sediment and water microbial communities to submerged vegetations restoration in a shallow eutrophic lake. *Sci. Total Environ.* 801, 149701 <https://doi.org/10.1016/J.SCITOTENV.2021.149701>.
- Clarkson, B., Ausseil, A., Gerbeaux, P., Dymond, J., 2013. In: Dymond, J.R. (Ed.), *Wetland Ecosystem Services*. Manaaki Whenua Press, Lincoln New Zealand.
- Costa, P.R., 2016. Impact and effects of paralytic shellfish poisoning toxins derived from harmful algal blooms to marine fish. *Fish. Fish.* 17, 226–248. <https://doi.org/10.1111/FAF.12105>.
- D'Auria, G., Barón-Rodríguez, M.M., Durbán-Vicente, A., Moya, A., Rojo, C., Latorre, A., Rodrigo, M.A., 2010. Unravelling the bacterial diversity found in the semi-arid Tablas de Daimiel National Park wetland (Central Spain). *Aquat. Microb. Ecol.* 59, 33–44. <https://doi.org/10.3354/AME01382>.

- Davidson, N.C., 2014. How much wetland has the world lost? Long-term and recent trends in global wetland area. *Mar. Freshw. Res.* 65, 934–941. <https://doi.org/10.1017/MF.14173>.
- de Carvalho, D.R., de Castro, D.M.P., Callisto, M., Moreira, M.Z., Pompeu, P.S., 2017. The trophic structure of fish communities from streams in the Brazilian Cerrado under different land uses: an approach using stable isotopes. *Hydrobiologia* 795, 199–217. <https://doi.org/10.1007/s10750-017-3130-6>.
- Dise, N.B., 2009. Peatland response to global change. *Science* (1979) 326, 810–811. doi: <https://doi.org/10.1126/science.1174268>.
- Duce, R.A., LaRoche, J., Altieri, K., Arrigo, K.R., Baker, A.R., Capone, D.G., Cornell, S., Dentener, F., Galloway, J., Ganeshram, R.S., Geider, R.J., Jickells, T., Kuypers, M.M., Langlois, R., Liss, P.S., Liu, S.M., Middelburg, J.J., Moore, C.M., Nickovic, S., Oschlies, A., Pedersen, T., Prospero, J., Schlitzer, R., Seitzinger, S., Sorensen, L.L., Uematsu, M., Ulloa, O., Voss, M., Ward, B., Zamora, L., 2008. Impacts of atmospheric anthropogenic nitrogen on the Open Ocean. *Science* 1979 (320), 893–897. <https://doi.org/10.1126/science.1150369>.
- Dudgeon, D., Arthington, A.H., Gessner, M.O., Kawabata, Z.I., Knowler, D.J., Leveque, C., Naiman, R.J., Prieur-Richard, A.H., Soto, D., Stiassny, M.L.J., Sullivan, C.A., 2006. Freshwater biodiversity: importance, threats, status and conservation challenges. *Biol. Rev.* 81, 163–182. <https://doi.org/10.1017/S1464793105006950>.
- Faust, K., 2021. Open challenges for microbial network construction and analysis. *ISME J.* <https://doi.org/10.1038/s41396-021-01027-4>.
- Feng, C., Jia, J., Wang, C., Han, M., Dong, C., Huo, B., Li, D., Liu, X., 2019. Phytoplankton and bacterial community structure in two chinese lakes of different trophic status. *Microorganisms* 7. <https://doi.org/10.3390/microorganisms7120621>.
- Hammer, D.A.T., Ryan, P.D., Hammer, Ø., Harper, D.A.T., 2001. Past: paleontological statistics software package for education and data analysis. *Palaeontol. Electron.* 4, 178.
- Horton, D.J., Theis, K.R., Uzarski, D.G., Learman, D.R., 2019. Microbial community structure and microbial networks correspond to nutrient gradients within coastal wetlands of the Laurentian Great Lakes. *FEMS Microbiol. Ecol.* 95, 33. <https://doi.org/10.1093/femsec/fiz033>.
- Kozich, J.J., Westcott, S.L., Baxter, N.T., Highlander, S.K., Schloss, P.D., 2013. Development of a dual-index sequencing strategy and curation pipeline for analyzing amplicon sequence data on the MiSeq Illumina sequencing platform. *Appl. Environ. Microbiol.* 79, 5112–5120. <https://doi.org/10.1128/AEM.01043-13>.
- Laguna, C., López-Perea, J.J., Viñuela, J., Florín, M., Feliu, J., Chicote, Á., Cirujano, S., Mateo, R., 2016. Effects of invasive fish and quality of water and sediment on macrophytes biomass, and their consequences for the waterbird community of a Mediterranean floodplain. *Sci. Total Environ.* 551–552, 513–521. <https://doi.org/10.1016/j.scitotenv.2016.02.059>.
- Li, H., Barber, M., Lu, J., Goel, R., 2020a. Microbial community successions and their dynamic functions during harmful cyanobacterial blooms in a freshwater lake. *Water Res.* 185, 116292. <https://doi.org/10.1016/j.watres.2020.116292>.
- Li, M., Mi, T., Yu, Z., Ma, M., Zhen, Y., 2020b. Planktonic bacterial and archaeal communities in an artificially irrigated estuarine wetland: diversity, distribution, and responses to environmental parameters. *Microorganisms* 8, 198. <https://doi.org/10.3390/MICROORGANISMS8020198>.
- Li, Y., Khan, F.H., Wu, J., Zhang, Y., Jiang, Y., Chen, X., Yao, Y., Pan, Y., Han, X., 2022. Drivers of spatiotemporal eukaryote plankton distribution in a Trans-Basin water transfer canal in China. *Front. Ecol. Evol.* 10. <https://doi.org/10.3389/fevo.2022.899993>.
- Llirós, M., Inceolu, Ö., García-Armisen, T., Anzil, A., Leporcq, B., Pigneur, L.M., Viroux, L., Darchambeau, F., Descy, J.P., Servais, P., 2014. Bacterial community composition in three freshwater reservoirs of different alkalinity and trophic status. *PLoS One* 9. <https://doi.org/10.1371/journal.pone.0116145>.
- Maggioni, L.A., Fontaneto, D., Bocchi, S., Gomasasca, S., 2009. Evaluation of water quality and ecological system conditions through macrophytes. *Desalination* 246. <https://doi.org/10.1016/j.desal.2008.03.052>.
- Moreno, L., Jiménez, M.E., 2013. Las Tablas de Daimiel National Park and Guadiana River peat fires of Spain. In: *Coal and Peat Fires: A Global Perspective*. Elsevier, pp. 427–440. <https://doi.org/10.1016/B978-0-444-59412-9.00022-3>.
- Newton, R.J., Jones, S.E., Eiler, A., McMahon, K.D., Bertilsson, S., 2011. A guide to the natural history of freshwater Lake Bacteria. *Microbiol. Mol. Biol. Rev.* 75, 14–49. <https://doi.org/10.1128/MMBR.00028-10>.
- OECD (Organization for Economic Cooperation and Development) (1982) Eutrophication of Waters. Monitoring Assessment and Control. Final Report. OECD Cooperative Programme on Monitoring of Inland Waters (Eutrophication Control), Environment Directorate, OECD, Paris, 154 p.
- Ortiz-Jiménez, M.A., De Anda, J., Shear, H., 2006. Nutrients/food chain model for Lake Zapotlan (Mexico). *Int. J. River Basin Manag.* 4, 125–135. <https://doi.org/10.1080/15715124.2006.9635282>.
- Pardo, L.H., Fenn, M.E., Goodale, C.L., Geiser, L.H., Driscoll, C.T., Allen, E.B., Baron, J.S., Bobbink, R., Bowman, W.D., Clark, C.M., Emmett, B., Gilliam, F.S., Greaver, T.L., Hall, S.J., Lilleskov, E.A., Liu, L., Lynch, J.A., Nadelhoffer, K.J., Perakis, S.S., Robin-Abbott, M.J., Stoddard, J.L., Weathers, K.C., Dennis, R.L., 2011. Effects of nitrogen deposition and empirical nitrogen critical loads for ecoregions of the United States. *Ecol. Appl.* 21, 3049–3082. <https://doi.org/10.1890/10-2341.1>.
- Parks, D.H., Chuvochina, M., Chaumeil, P.-A., Rinke, C., Mussig, A.J., Hugenholtz, P., 2019. Selection of representative genomes for 24,706 bacterial and archaeal species clusters provide a complete genome-based taxonomy. *BioRxiv* 771964. <https://doi.org/10.1101/771964>.
- Quast, C., Pruesse, E., Yilmaz, P., Gerken, J., Schweer, T., Yarza, P., Peplies, J., Glöckner, F.O., 2013. The SILVA ribosomal RNA gene database project: improved data processing and web-based tools. *Nucleic Acids Res.* 41, D590–D596. <https://doi.org/10.1093/NAR/GKS1219>.
- Rousoo, B.Z., Bertone, E., Stewart, R.A., Rinke, K., Hamilton, D.P., 2021. Light-induced fluorescence quenching leads to errors in sensor measurements of phytoplankton chlorophyll and phycocyanin. *Water Res.* 198, 117133. <https://doi.org/10.1016/j.watres.2021.117133>.
- Sánchez-Carrillo, S., Reddy, K.R., Inglett, K.S., Álvarez-Cobelas, M., Sánchez-Andrés, R., 2014. Biogeochemical indicators of nutrient enrichments in wetlands: the microbial response as a sensitive indicator of wetland eutrophication. *Eutrophication: Causes, Consequences and Control*. https://doi.org/10.1007/978-94-007-7814-6_15.
- Santofimia, E., López Pamo, E., González Toril, E., Mejías Moreno, M., Ruiz, J.M., Aguilera, A., 2021. Parque Nacional Tablas de Daimiel: El humedal frente a la actividad de las especies exóticas invasoras, la turbidez y la eutrofización. In: *Geotemas (Madrid)*. Sociedad Geológica de España, pp. 325–326. ISSN 1576–5172, No. 18, 2021 (X Congreso Geológico de España), Pág. 325.
- Schloss, P.D., Westcott, S.L., Ryabin, T., Hall, J.R., Hartmann, M., Hollister, E.B., Lesniewski, R.A., Oakley, B.B., Parks, D.H., Robinson, C.J., Sahl, J.W., Stres, B., Thallinger, G.G., Van Horn, D.J., Weber, C.F., 2009. Introducing mothur: open-source, platform-independent, community-supported software for describing and comparing microbial communities. *Appl. Environ. Microbiol.* 75, 7537–7541. <https://doi.org/10.1128/AEM.01541-09>.
- Schwarz, A.M., Hawes, I., 1997. Effects of changing water clarity on characean biomass and species composition in a large oligotrophic lake. *Aquat. Bot.* 56. [https://doi.org/10.1016/S0304-3770\(96\)01114-X](https://doi.org/10.1016/S0304-3770(96)01114-X).
- Tas, B., 2011. Bloom and eutrophication of *Hydrodictyon reticulatum* (Chlorophyceae) at civil and Kacali stream, Ordu, Turkey. *Energy Sci. Res.* 28, 319–330.
- Urakawa, H., Bernhard, A.E., 2017. Wetland management using microbial indicators. *Ecol. Eng.* 108, 456–476. <https://doi.org/10.1016/j.ecoleng.2017.07.022>.
- van Asselen, S., Verburg, P.H., Vermaat, J.E., Janse, J.H., 2013. Drivers of wetland conversion: a global meta-analysis. *PLoS One* 8, e81292. <https://doi.org/10.1371/journal.pone.0081292>.
- Veira, J., Necchi, O., 2003. Photosynthetic characteristics of charophytes from tropical lotic ecosystems. *Phycol. Res.* 51, 51–60. <https://doi.org/10.1046/J.1440-1835.2003.00293.X>.
- Wang, B., Ma, B., Stirling, E., He, Z., Zhang, H., Yan, Q., 2023. Freshwater trophic status mediates microbial community assembly and interdomain network complexity. *Environ. Pollut.* 316, 120690. <https://doi.org/10.1016/j.envpol.2022.120690>.
- Wang, H., Liu, C., Yu, D., 2015. Morphological and reproductive differences among three charophyte species in response to variation in water depth. *Aquat. Bot.* 24, 91–100. <https://doi.org/10.3354/AB00638>.
- Wang, Y., Chen, L., Niu, Y., Yu, H., Luo, M., 2016. Spatio-temporal variation in phytoplankton community and its influencing factors in Danjiangkou reservoir. *Hupo Kexue/J. Lake Sci.* 28, 1057–1065. <https://doi.org/10.18307/2016.0516>.
- Wang, Y., Guo, M., Li, X., Liu, G., Hua, Y., Zhao, J., Huguet, A., Li, S., 2022. Shifts in microbial communities in shallow lakes depending on trophic states: feasibility as an evaluation index for eutrophication. *Ecol. Indic.* 136, 108691. <https://doi.org/10.1016/j.ecolind.2022.108691>.
- Ward, Tockner, 2001. Biodiversity: towards a unifying theme for river ecology. *Freshw. Biol.* 46, 807–819. <https://doi.org/10.1046/J.1365-2427.2001.00713.X>.
- Xiaoran, O., Qiaohua, Z., Yingzhu, W.E.I., 2013. A preliminary exploration of dissolved oxygen based on FVCOM in Meiliang Bay, Lake Taihu and its influence mechanism. *J. Lake Sci.* 25, 478–488. doi:10.18307/2013.0404.
- Xie, G., Tang, X., Gong, Y., Shao, K., Gao, G., 2020. How do planktonic particle collection methods affect bacterial diversity estimates and community composition in oligo-, meso- and eutrophic lakes? *Front. Microbiol.* 11, 593589. <https://doi.org/10.3389/FMICB.2020.593589/BIBTEX>.
- Yilmaz, P., Parfrey, L.W., Yarza, P., Gerken, J., Pruesse, E., Quast, C., Schweer, T., Peplies, J., Ludwig, W., Glöckner, F.O., 2014. The SILVA and “all-species living tree project (LTP)” taxonomic frameworks. *Nucleic Acids Res.* 42, D643–D648. <https://doi.org/10.1093/nar/gkt1209>.
- Zuur, A.F., Ieno, E.N., Smith, G.M., 2007. Analyzing ecological data. *Methods*. <https://doi.org/10.1016/B978-0-12-387667-6.00013-0>.